Structural and electronic properties of zinc blende-type nitrides BxAl1–xN

Rabah Riane, Zouaoui Boussahl, Samir F. Matar, Ali Zaoui

Structural and Electronic Properties of Zinc Blende-type Nitrides $B_xAl_{1-x}N$

Rabah Riane[a], Zouaoui Boussahla[a], Samir F. Matar[b], and Ali Zaoui[a]

[a] Modelling and Simulation in Materials Science Laboratory, Physics Department, University of Sidi Bel-Abbes, 22000 Algeria
[b] CNRS, ICMCB, University of Bordeaux 1, 87 Avenue Dr. Albert Schweitzer, 33600 Pessac, France

Reprint requests to Dr. S. F. Matar. E-mail: matar@icmcb-bordeaux.cnrs.fr

Z. Naturforsch. **2008**, *63b,* 1069 – 1076; received April 8, 2008

First principles total energy calculations were carried out to investigate structural and electronic properties of zinc blende-type AlN, BN and $B_xAl_{1-x}N$ solid solutions. We have calculated the lattice parameters, bulk modulus, pressure derivative, and $B_xAl_{1-x}N$ band-gap energy for zinc blende-type crystals of the compositions x = 0, 0.25, 0.5, 0.75, 1. The results show that the direct energy gap $\Gamma_{15}^{v} \rightarrow \Gamma_{1}^{c}$ shows a strong nonlinear dependence on the concentration x. For high boron contents ($x > 0.71$), these materials have a phase transition from direct-gap semiconductors to indirect-gap semiconductors ($\Gamma_{15}^{v} \rightarrow X_{1}^{c}$). This essential feature indicates that these materials should have very good optical properties at high concentrations of boron compared to those of AlN. Further discussions concern a comparison of our results with results obtained with other available theoretical and experimental methods.

Key words: DFT, Wide-gap Semiconductors, FP-LAPW

Introduction

Semiconductors of binary nitrides such as AlN, GaN, InN, or BN are of great interest and are widely used for the fabrication of optical and electronic devices. In the last decade many investigations were devoted to the study of structural and electronic properties of wide-gap semiconductors [1, 2]. Regarding ternary nitride semiconductors, different studies were dedicated to the calculation of the structural and electronic properties of these materials [3 – 12]. The electronic behavior such as the band-gap width can be tuned by substitution. The purpose of this paper is to illustrate such modifications by providing original *ab initio* data on the structural and electronic properties of zinc blende-type $B_xAl_{1-x}N$ solid solutions with different compositions, x = 0, 0.25, 0.50, 0.75, and 1, and compare them with zinc blende-type AlN and BN. The calculations were carried out within the density functional theory (DFT) [13, 14].

Method of Calculation

Self-consistent calculations of total energies and the electronic structure based on the scalar relativistic full-potential (FP) "linearized augmented plane wave" (LAPW) method were carried out using the WIEN2K code [15]. This is a very accurate and efficient scheme to solve the Kohn-Sham equations of density functional theory (DFT). While this method can use different schemes for the treatment of the effects of exchange and correlation, we here use, like in former work [1, 2], the local density approximation (LDA) following the Perdew-Wang implementation [16]. Basis functions, electron densities and potentials were expanded inside the muffin-tin (MT) spheres in combination with spherical harmonic functions with a cutoff l_{max} = 10, and in Fourier series in the interstitial region. Within this method a parameter which determines the matrix size, $R_{MT}K_{max}$, was used with a value of 7, where R_{MT} denotes the atomic sphere radius, and K gives the magnitude of the K_{max} vector in the plane wave expansion.

For AlN we adopted the values of 1.75 and 1.6 Bohr (1 Bohr = 0.529 Å) for aluminum and nitrogen, respectively, as the MT radii. In the case of BN we used 1.32 and 1.45 Bohr for boron and nitrogen, respectively.

For modelling the $B_xAl_{1-x}N$ solid solutions, we have chosen the MT radii values of 1.7, 1.5 and 1.4 Bohr for aluminum, nitrogen, and boron, respectively. In the calculations, we have distinguished the Al ($1s^2\,2s^2\,2p^6$), N ($1s^2$) and B ($1s^2$) inner-shell electrons from the valence electrons of Al ($3s^2\,3p^1$), N ($2s^2\,2p^3$) and B ($2s^2 2p^1$) shells. For the irreducible

Table 1. Lattice constants a, bulk modulus B, and pressure derivative of bulk modulus B' for zinc blende-type AlN, BN and $B_xAl_{1-x}N$ solid solutions.

Composition		This work LDA	Other theoretical studies	Experimental data
AlN	a, Å	4.34	4.349[a]; 4.35[b]	4.38[c]
	B, GPa	209	211.78[a]; 209[b]	
	B', GPa	3.38	3.90[a]; 3.89[b]	
$B_{0.25}Al_{0.75}N$	a, Å	4.20		
	B, GPa	235		
	B', GPa	4.53		
$B_{0.5}Al_{0.5}N$	a, Å	4.04		
	B, GPa	266		
	B', GPa	3.56		
$B_{0.75}Al_{0.25}N$	a, Å	3.84		
	B, GPa	318		
	B', GPa	2.95		
BN	a, Å	3.58	3.354[a]; 3.623[d]; 3.66[e]	3.615[f]
	B, GPa	404	401.7[a]; 368[d]; 353[e]	382; 400[g]
	B', GPa	3.42	3.66[a]; 3.32[d]	3.0; 4.0[g]

[a] Ref. [2]; [b] ref. [19]; [c] ref. [20]; [d] ref. [21]; [e] ref. [22]; [f] ref. [23]; [g] ref. [24].

wedge of the Brillouin zone, a mesh of 10 special k-points for the binary cases, and eight special k-points were used for the supercell calculations.

Calculations and Results

Structural properties

First calculations were carried out to determine the structural properties of zinc blende-type AlN and BN and of $B_xAl_{1-x}N$ solid solutions.

To model the $B_xAl_{1-x}N$ zinc blende solid solutions, we applied a 32-atom $B_nAl_{16-n}N_{16}$ supercell, which corresponds to $2 \times 2 \times 1$ single cells. For the considered structures and at different boron concentrations x (x = 0, 0.25, 0.50, 0.75, 1), the structural properties were obtained by a minimization of the total energy as a function of the volume for AlN, BN and $B_xAl_{1-x}N$ in the zinc blende structure. The bulk moduli and their pressure derivatives were obtained by a non-linear fit of the total energy *versus* volume according to the Birch-Murnaghan equation of state [17]. In Table 1, we summarize the calculated structural properties (lattice parameters, bulk moduli and their pressure derivatives) of AlN, BN and $B_xAl_{1-x}N$ solid solutions together with available theoretical and experimental data from the literature. The analysis of our computed quantities shows a good agreement with published results [2, 19 – 24].

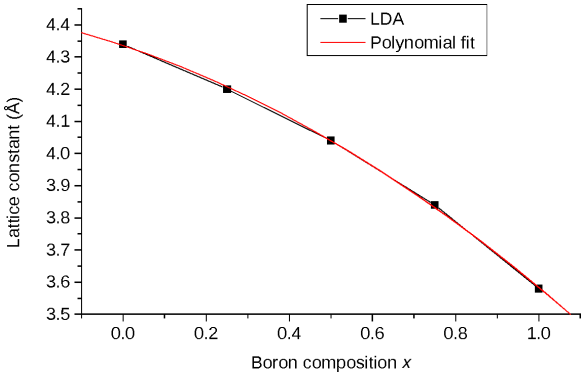

Fig. 1. The lattice parameter of $B_xAl_{1-x}N$ as a function of the boron composition.

Assuming that Vegard's law is valid, the lattice parameters of the $B_xAl_{1-x}N$ solid solutions are generally expressed as a linear relation of the boron concentration x [18], as given in Eq. 1:

$$a(x) = x a_{BN} + (1-x) a_{AlN} \tag{1}$$

Then we tested the validity of Vegard's law for the ternary $B_xAl_{1-x}N$ compounds with a zinc blende structure with different boron concentrations, x = 0, 0.25, 0.5, 0.75 and 1. The results are plotted in Fig. 1. To analyze the degree of deviation from Vegard's law, the lattice parameter of the $B_xAl_{1-x}N$ solid solutions as a function of the boron composition x can be approximated using the following formula (Eq. 2):

$$a(x) = x a_{BN} + (1-x) a_{AlN} - x(1-x) b, \tag{2}$$

where $a(x)$ is the composition-dependent lattice parameter of the $B_xAl_{1-x}N$ solutions, a_{BN} and a_{AlN} the lattices parameters of BN and AlN, respectively, and b the deviation parameter of the lattice parameter. With the best fit of the results shown in Fig. 1 using Eq. 2, we found the deviation parameter of the lattice parameter $b = -0.32$. For AlN and BN, we found an underestimation of the lattice parameters when we compare these results to the available experimental data [20, 23]. This can be interpreted by the use of the LDA in the calculations which is known to be overbinding. In Fig. 2 we plot the results of the bulk moduli *versus* composition for $B_xAl_{1-x}N$. Between the different values of the bulk modulus of the pristine extreme binary nitrides, AlN and BN, we observed a nonlinear increase with x of the bulk modulus within the $B_xAl_{1-x}N$ solid solution. This could be due to the approximation made to simulate the ternary $B_xAl_{1-x}N$ system within an ordered

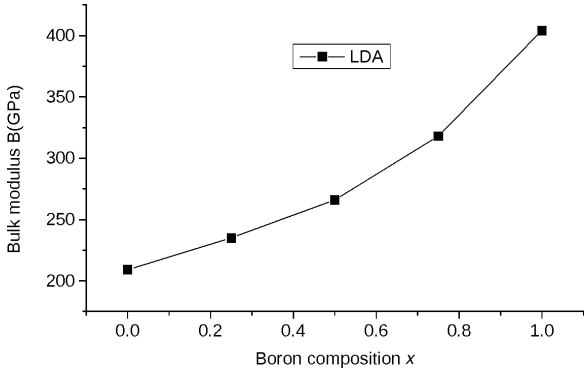

Fig. 2. Composition dependence of the calculated modulus for the solid solutions.

supercell. Solid solution calculations assuming disorder can be better carried out using a coherent potential approximation (CPA) [25].

Electronic structures

The calculations of the electronic band structures, the magnitude of the band gap and the density of states were carried out for AlN, BN and $B_xAl_{1-x}N$ zinc blende structures at the equilibrium-calculated lattice parameters. The energies calculated using the FP-LAPW method for zinc blende-type AlN and BN are listed in Table 2 for the high-symmetry points Γ, X and L in the Brillouin zone. The results are in agreement with previous reports [19–26]. All energies are with reference to the top of the valence band Γ_{15}^{v}. The

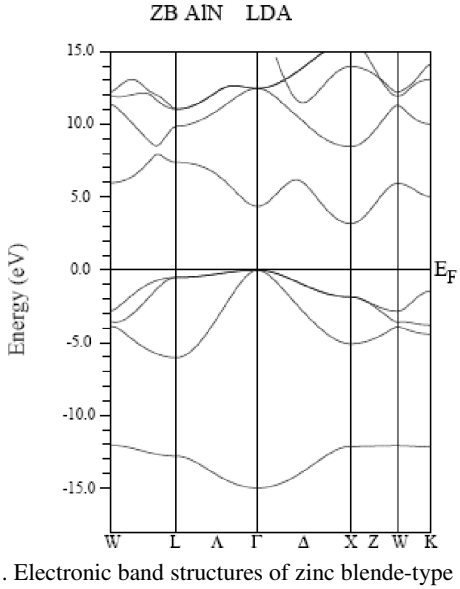

Fig. 3. Electronic band structures of zinc blende-type AlN.

Table. 2. Zinc blende-type AlN and BN: Energies in eV at high symmetry points in the Brillouin zone. All values refer to the top of the valence band.

High symmetry points	AlN	BN
Γ_1^v	−14.9	−20.38
Γ_{15}^v	0.02	0.00
Γ_1^c	4.32	8.77
Γ_{15}^c	12.47	10.81
X_1^v	−12.10	−14.56
X_3^v	−5.00	−9.07
X_5^v	−1.80	−5.06
X_1^c	3.19	4.34
X_3^c	8.47	9.26
X_5^c	14.00	18.10
L_1^v	−12.79	−16.04
L_1^v	−6.02	−10.96
L_3^v	−0.50	−2.00
L_1^c	7.39	10.50
L_3^c	9.87	10.68
L_1^c	11.04	15.27

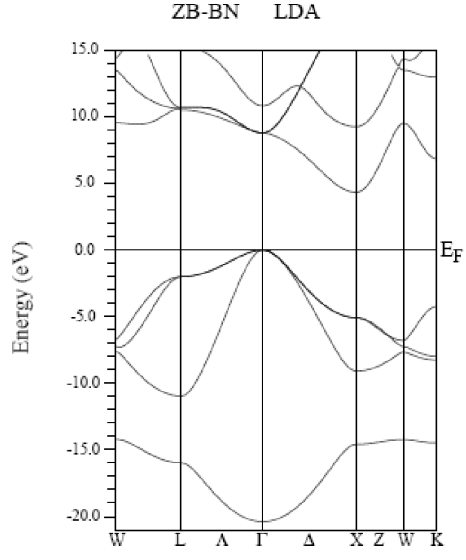

Fig. 4. Electronic band structures of zinc blende-type BN.

electronic structures of AlN and BN along the symmetry lines are shown in Figs. 3 and 4, respectively. The results show that zinc blende-type AlN and BN are indirect-gap semiconductors with the minimum of the conduction band at the X_1^c point. The calculated energy gaps of AlN and BN, E_g^x, 3.21 and 4.35 eV, respectively, are in good agreement with the theoretical values as listed in Table 3 [19–26].

Focusing on the electronic properties of the $B_xAl_{1-x}N$ ternary system, we obtained direct band gaps for the transition from the valence-band maximum (Γ_{15}^v point) to the conduction band Γ_1^c points.

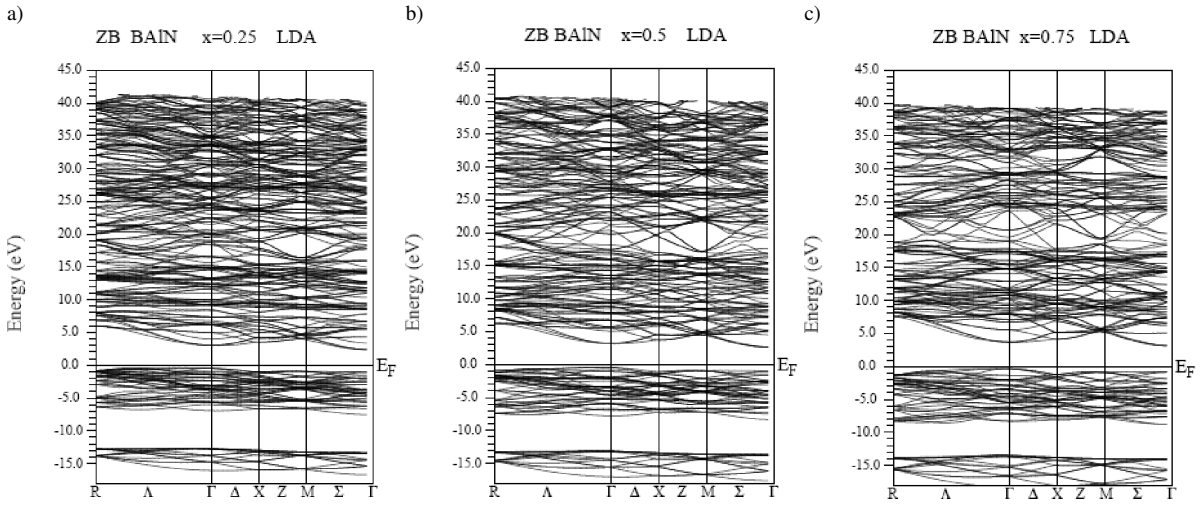

Fig. 5. The band structure of zinc blende-type $B_xAl_{1-x}N$: a) $x = 0.25$, b) $x = 0.5$, c) $x = 0.75$. E_F refers here to the top of the valence band.

Table 3. Summary of the band gaps and total valence band widths of compounds BN and AlN and zinc blende-type $B_xAl_{1-x}N$ solid solutions (energies in eV).

Composition		This work LDA	Other theoretical studies	Experimental data
AlN	$E_g(\Gamma_{15}^v \to \Gamma_1^c)$	4.37	4.32[a]; 4.2[b]	
	$E_g(\Gamma_{15}^v \to X_1^c)$	3.21	3.21[a]; 3.2[b]	5.34[c]
	Total valence bandwidth	14.92	14.92[a]; 14.8[b]	
$B_{0.25}Al_{0.75}N$	$E_g(\Gamma_{15}^v \to \Gamma_1^c)$	3.48		
	$E_g(\Gamma_{15}^v \to X_1^c)$	4.16		
	Total valence bandwidth	18.30		
$B_{0.5}Al_{0.5}N$	$E_g(\Gamma_{15}^v \to \Gamma_1^c)$	3.63		
	$E_g(\Gamma_{15}^v \to X_1^c)$	4.35		
	Total valence bandwidth	16.64		
$B_{0.75}Al_{0.25}N$	$E_g(\Gamma_{15}^v \to \Gamma_1^c)$	4.04		
	$E_g(\Gamma_{15}^v \to X_1^c)$	4.69		
	Total valence	17.98		
BN	$E_g(\Gamma_{15}^v \to \Gamma_1^c)$	8.78	8.79[d]	14.50[e]
	$E_g(\Gamma_{15}^v \to X_1^c)$	4.35	4.35[d]	6.00[f]
	Total valence bandwidth	20.38	20.35[d]	22.00[f]

[a] Ref. [19]; [b] ref. [26]; [c] ref. [27]; [d] ref. [21]; [e] ref. [28]; [f] ref. [29].

The electronic band structure of zinc blende-type $B_xAl_{1-x}N$ is shown in Fig. 5. The total bowing parameter is calculated by fitting the nonlinear variation of the calculated direct and indirect band gaps in terms of concentration with a polynomial function.

The results are shown in Fig. 6 and obey the following variations (Eqs. 3, 4):

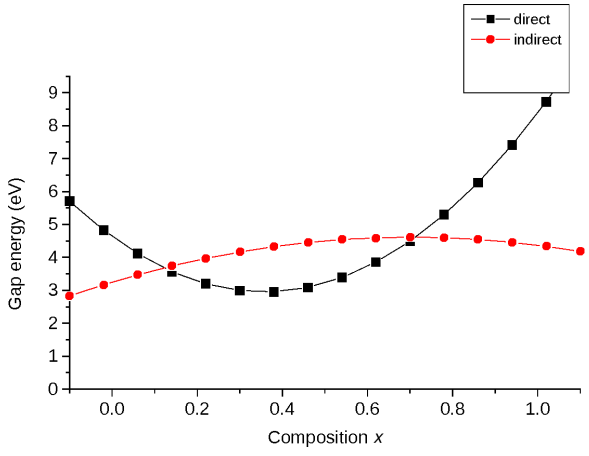

Fig. 6. Composition dependence of the direct ($\Gamma_{15}^v \to \Gamma_1^c$) and indirect ($\Gamma_{15}^v \to X_1^c$) band gaps in zinc blende-type $B_xAl_{1-x}N$.

Direct gap

$$E_{\Gamma\to\Gamma} = 4.629 - 9.413x + 13x^2 \tag{3}$$

Indirect gap

$$E_{\Gamma\to X} = 3.242 + 3.901x - 2.777x^2 \tag{4}$$

The values of E_g deviate from linear behavior. This deviation is characterized by the bowing parameter b. We found $b = 13.16$ and -2.77 eV for the ($\Gamma_{15}^v \to \Gamma_1^c$) and ($\Gamma_{15}^v \to X_1^c$) transitions, respectively. Because the shift between the lattice parameters of BN and AlN is larger than 10 %, one must expect an important disorder in

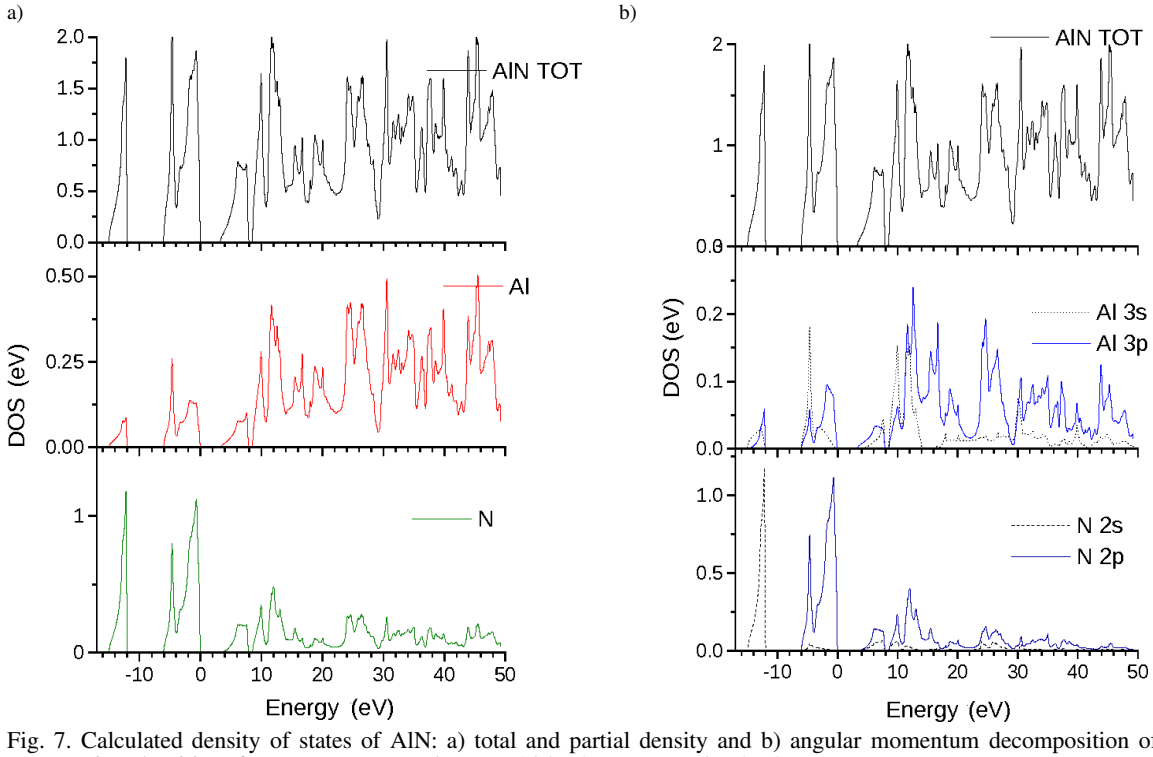

Fig. 7. Calculated density of states of AlN: a) total and partial density and b) angular momentum decomposition of the atom-project densities of states. From top to bottom: Al 3*s*, 3*p* states, and N 2*s*, 2*p* states.

the electronic and structural properties. Hence it is advisable to work in constrained mode and not in pseudomorphic mode. Then, the bowing for the ($\Gamma_{15}^{v} \rightarrow \Gamma_{1}^{c}$) point transition is larger than for the ($\Gamma_{15}^{v} \rightarrow X_{1}^{c}$) point transition. The indirect to direct band gap transition is predicted to occur at two points, namely $x = 0.12$ and $x = 0.71$. We found that the fluctuations of the energy gap are pronounced for the ($\Gamma_{15}^{v} \rightarrow \Gamma_{1}^{c}$) transition, while for the $\Gamma_{15}^{v} \rightarrow X_{1}^{c}$ point they are small. Also, the band gap energy widths for the $B_xAl_{1-x}N$ solid solutions are larger than those of AlN and increase monotonically.

Density of states (DOS)

An essential ingredient in determining the electronic properties of solids is the energy distribution of the valence- and conduction-band electrons.

Theoretical quantities such as the total electronic energy of a solid, the position of the Fermi level, and the tunnelling probabilities of electrons call for detailed calculations of the electronic density of state (DOS). Calculations of the DOS require a very high degree of precision with the use of a fine k-point mesh in the first Brillouin zone (BZ). In our calculations we considered a k-mesh = 3000 for AlN and BN, and a k-mesh = 100 for the $B_{0.25}Al_{0.75}N$ solid solutions. For zinc blende-type AlN and BN the total DOS presents three regions. Two valence regions, VB1 and VB2, below the top of the valence band E_F, and one conduction band CB above E_F (Figs. 7a and 8a). The lower VB2 valence-band region is dominated by N 2*s* states and the upper VB1 valence band by N $2p^3$ and Al $3p^1$ states for AlN, and by N $2p^3$, $2p^1$ states for BN. The Al 3*s* and B 2*s* states contribute to the lowest valence bands. The first conduction band is predominantly of Al $3s^2$ and B $2s^2$ character. For the purpose of providing a qualitative explanation of these contributions, Figs. 7b and 8b show the angular momentum decomposition of the atom-projected DOS of AlN and BN, used to analyze the orbital character of different states.

It is also desirable to determine the type of hybridization of the states responsible for the bonding.

The shape of the DOS (Figs. 7 and 8) showing similar skylines is due of the chemical bonding between Al and N involving Al 3*s* and 3*p* and N 2*s* and 2*p* orbitals, and between B and N involving B 2*s* and 2*p* with

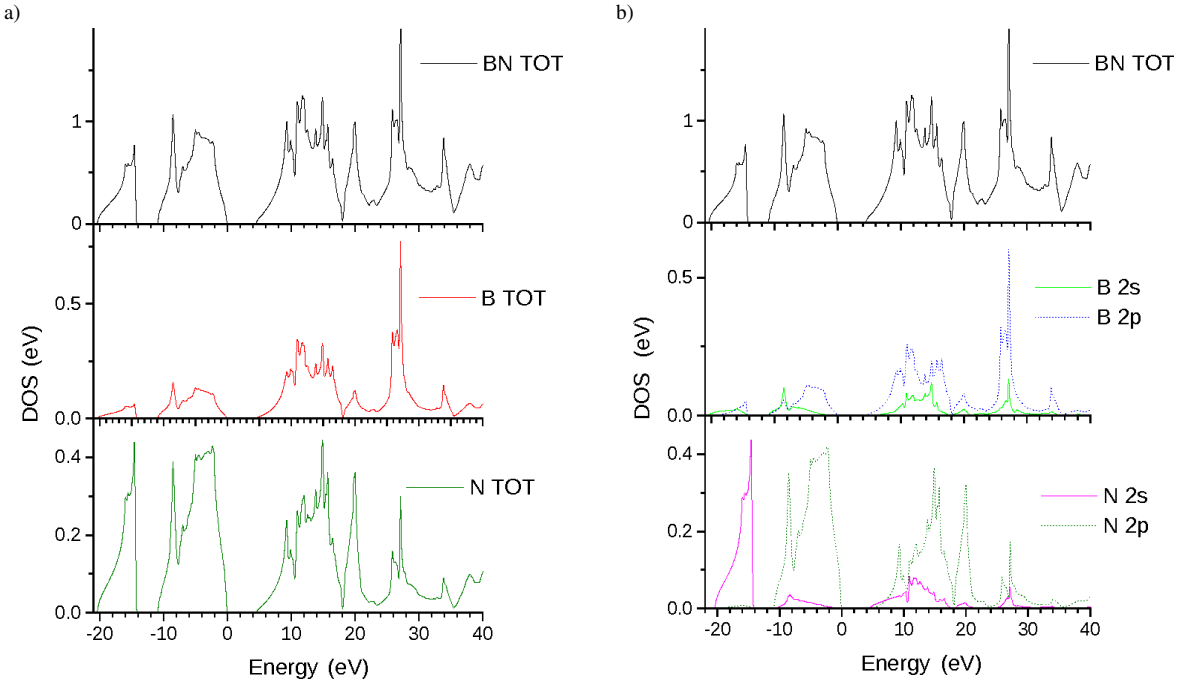

Fig. 8. Calculated density of states of BN: a) total and partial density and b) angular momentum decomposition of the atom-project densities of states. From top to bottom: B 2*s*, 2*p* states, and N 2*s*, 2*p* states.

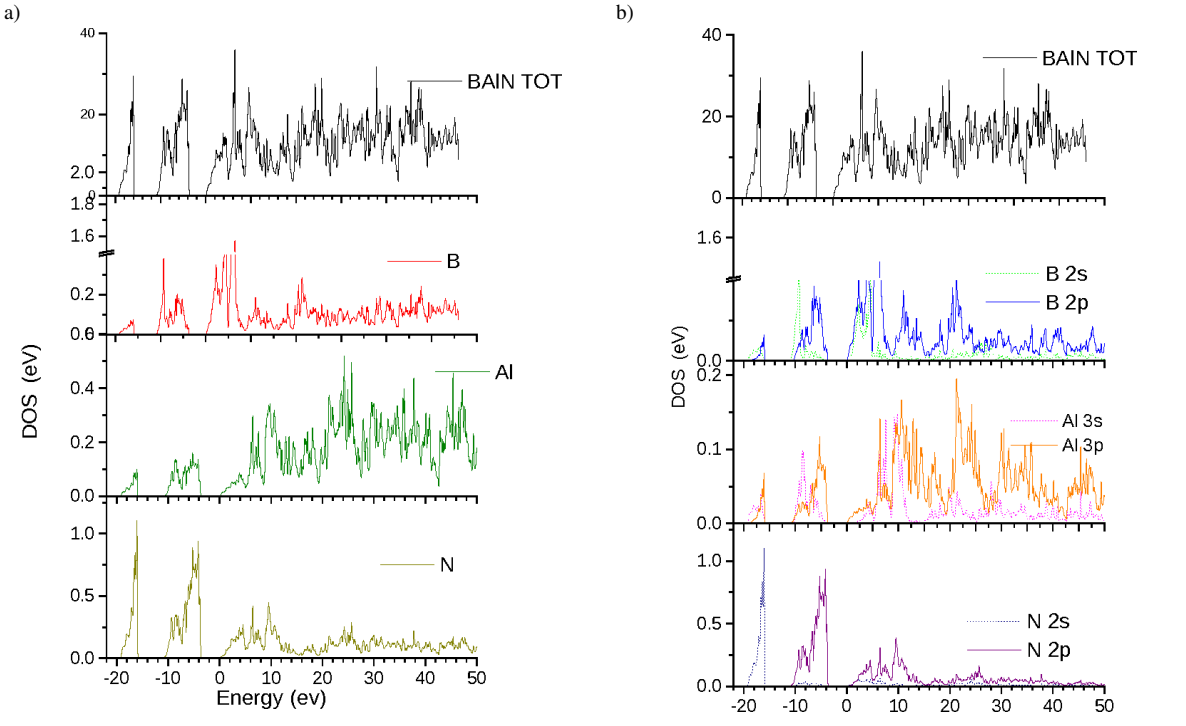

Fig. 9. Calculated density of states $B_{0.25}Al_{0.75}N$: a) total and partial density and b) angular momentum decomposition of the atom-project densities of states. From top to bottom: B 2*s*, 2*p*, Al 3*s*, 3*p* states, and N 2*s*, 2*p* states.

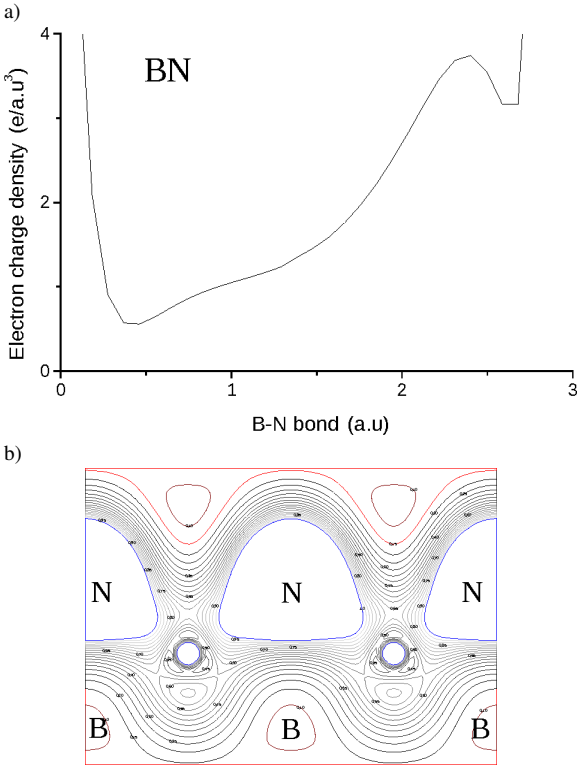

Fig. 10. (Color online). Total valence charge densities in zinc blende-type BN: a) along the (111) direction and b) in the plane (110).

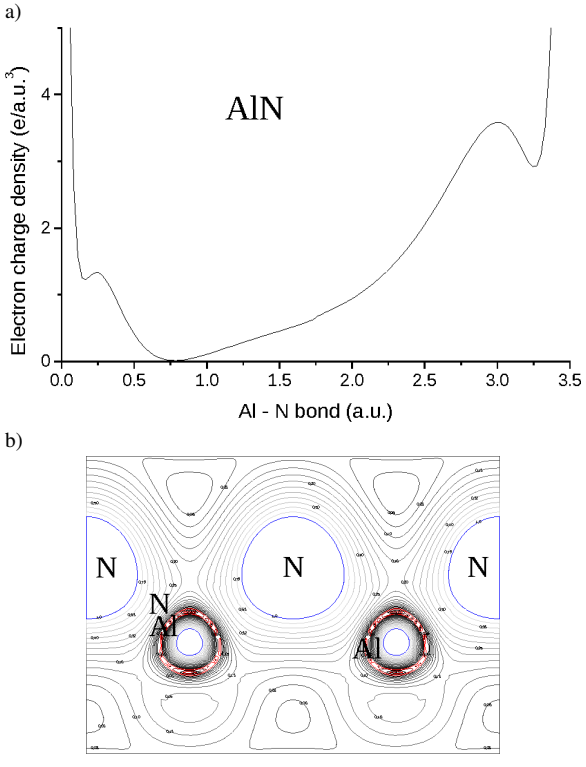

Fig. 11. (Color online). Total valence charge densities in AlN: a) along the (111) direction and b) in the plane (110).

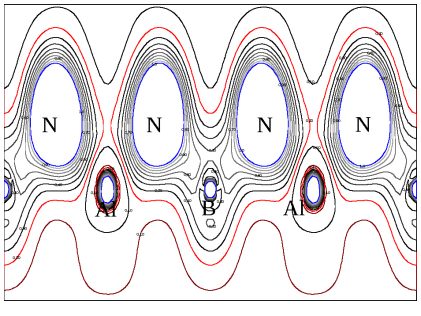

Fig. 12. (Color online). Total valence charge densities in zinc blende-type $B_{0.25}Al_{0.75}N$ in the plane (110).

N 2*s* and 2*p* orbitals. This interaction is especially pronounced between the N 2*p* and Al 3*p* orbitals which are more directional. The total and partial density of states of $B_{0.25}Al_{0.75}N$ shown in Fig. 9a is an essential feature to study the nature of chemical bonding in these materials: the first peak at the bottom of the valence band originates from the contribution of N *s* states, followed at higher energy (~ -16 eV) by B *s* states. The reason for this is the difference in electronegativity between N and B. This leads to a charge transfer from boron to nitrogen and explains the occurrence of the first peak in $B_{0.25}Al_{0.75}N$. This feature is further confirmed by the electronic charge density of $B_{0.25}Al_{0.75}N$ (Fig. 12), where the contours around N exhibit a higher charge than at the boron site.

Total valence charge densities

To visualize the nature of the bond character, and to explain the charge transfer and the bonding properties of AlN, BN and their solid solutions $B_{0.25}Al_{0.75}N$ and $B_{0.5}Al_{0.5}N$, we calculated the total valence charge density. We show in Figs. 10 – 12 the total valence charge densities along the [111] direction and in the (110) plane for each material. The calculated electronic charge distribution indicates that there is a strong ionic character of the Al–N and B–N bonds. The nitrogen ions are larger than the aluminum (boron) ions in both cases. The driving force behind the displacement of the charge is the greater ability of N to attract electrons due to the difference in the electronegativity of Al and N and of B and N. Because of the large mixing of the

wave functions for $B_{0.25}Al_{0.75}N$ and $B_{0.5}Al_{0.5}N$, these compounds have the same charge densities whose characteristics are intermediate between those of AlN and BN.

Conclusion

In this paper we report on a computational study of structural and electronic properties of zinc blende-type AlN and BN and of $B_xAl_{1-x}N$ solid solutions. The calculated lattice parameters, bulk moduli and band gaps E_g of the binary compounds agree well with results of other theoretical calculations. The calculated structural and electronic properties of the $B_xAl_{1-x}N$ solid solutions for different boron compositions x show that E_g for $(\Gamma_{15}^v \rightarrow \Gamma_1^c)$ has a strong nonlinear dependence on the concentration x. For high concentrations of boron, $x > 0.71$, these materials have a phase transition from a direct-gap $(\Gamma_{15}^v \rightarrow \Gamma_1^c)$ semiconductor to an indirect-gap semiconductor at the $(\Gamma_{15}^v \rightarrow X_1^c)$ point, and this essential feature indicates that these materials have very good optical properties at high concentrations of boron compared to those of AlN. According to our calculations materials with $x = 0.5$ and $x = 1$ have the same energy $E_{\Gamma-X} = 4.35$ eV so that the optical properties can be expected to be the same. Also for $Al_{0.25}B_{0.75}N$, the bulk modulus B is large, and the lattice parameter a is relatively small compared to that of AlN, which supports the use of these materials in thin layer electronic devices.

[1] V. Serin, C. Colliex, R. Brydson, S. Matar, F. Boucher, *Phys. Rev. B* **1998**, *58*, 5106.

[2] M. B. Kanoun, A. E. Merad, J. Cibert, H. Aourag, *Solid State Electronics* **2004**, *48*, 1601.

[3] V. V. IIyasov, T. P. Zhadanova, I. Y. Nikiforov, *Phys. Solid State* **2006**, *48*, 213.

[4] V. V. IIyasov, T. P. Zhadanova, I. Y. Nikiforov, *Phys. Solid State* **2006**, *48*, 654.

[5] V. V. IIyasov, T. P. Zhadanova, I. Y. Nikiforov, *Phys. Solid State* **2005**, *47*, 1618.

[6] T. P. Zhadanova, V. V. IIyasov, I. Y. A. Nikiforov, *Phys. Solid State* **2001**, *43*, 1445.

[7] L. K. Teles, L. M. R. Scolfaro, J. R. Leite, J. Furthmüller, F. Bechstedt, *Appl. Phys. Lett*. **2002**, *80*, 1177.

[8] L. K. Teles, J. Furthmüller, L. M. R. Scolfaro, A. Tabata, J. R. Leite, F. Bechstedt, T. Frey, D. J. As, K. Lischka, *Physica E* **2002**, *13*, 1086.

[9] T. Honda, M. Shibata, M. Kurimoto, M. Tsubamoto, J. Yamamoto, H. Kawanishi, *Jap. J. Appl. Phys*. **2000**, *39*, 2389.

[10] S. Azzia, A. Zaoui, M. Ferhat, *Solid State Commun.* **2007**, *144*, 245.

[11] L. Escalanti, G. L. W. Hart, *Appl. Phys. Lett*. **2004**, *84*, 705.

[12] V. Ilyasov, T. Zhdanova, I. Nikiforov, *Acta Crystallogr*. **2006**, *A62*, s62.

[13] P. Hohenberg, W. Kohn, *Phys. Rev. B* **1964**, *136*, 864.

[14] W. Kohn, L. J. Sham, *Phys. Rev*. **1965**, *140*, A1133.

[15] P. Blaha, K. Schwarz, G. K. H. Madser, D. Kvasnicka, J. Luitz, Wien2k, An Augmented Plane Wave plus Local Orbital Program for Calculating Crystal Properties, Vienna University of Technology, Vienna (Austria) **2001**.

[16] P. Perdew, S. Burke, M. Ernzerhof, *Phys. Rev. Lett*. **1996**, *77*, 3865.

[17] F. D. Murnaghan, *Proc. Natl. Acad. Sci. U.S.A*. **1947**, *30*, 244; J. R. Macdonald, D. R. Powell, *J. Res. Natl. Bur. Stand., Sect. A* **1971**, *75*, 441.

[18] L. Vegard, *Z. Phys*. **1921**, *5*, 17.

[19] Z. Boussahla, B. Abbar, B. Bouhafs, A. Tadjer, *J. Solid State Chem*. **2005**, *178*, 2117.

[20] A. Trampert, O. Brandt, K. H. Ploog in *Gallium Nitride I, Semiconductors and Semimetals*, Vol. 50 (Eds: J. L. Pankove, T. D. Moustakas), Academic Press, San Diego **1998**, p. 167.

[21] A. Zaoui, F. El Haj Hassan, *J. Phys. Condens. Matter* **2001**, *13*, 253.

[22] S. Matar, V. Gonnet, G. Demazeau, *J. Phys. I France* **1994**, *4*, 335.

[23] V. L. Solozhenho in *Properties of Group III Nitrides*, (Ed.: J. H. Edgar), INSPEC Publications, London **1994**, p. 43.

[24] M. Grimsditch, E. S. Zouboulis, A. Polian, *J. Appl. Phys*. **1994**, *76*, 832.

[25] A. M. N. Niklasson, J. M. Wills, M. I. Katsnelson, I. A. Abrikosov, O. Eriksson, B. Johannsson, *Phys. Rev. B* **2003**, *67*, 235105.

[26] F. Litimien, B. Bouhafs, Z. Dyridi, P. Ruterana, *New Journal of Phys*. **2002**, *64*,1.

[27] M. P. Thompson, G. W. Auner, T. S. Zheleva, K. A. Jones, S. J. Simko, J. N. Hilfiker, *J. Appl. Phys*. **2001**, *89*, 3331.

[28] O. Madelung (Ed.), *Physics of Group IV Elements and III-V Compounds, Numerical Data and Functional Relationship in Science and Technology, Landolt-Börnstein, New Series*, Group III, Vol. 17, Subvolume a, Springer, Berlin **1982**.

[29] V. A. Fomichev, M. A. Rumsh, *J. Chem. Phys.* **1968**, *48*, 555; V. A. Fomichev, M. A. Rumsh, *J. Phys. Chem. Solids* **1968**, *29*, 1015.